Cellular and Molecular Life Sciences (2026) 83:188
https://doi.org/10.1007/s00018-026-06177-2

ORIGINAL ARTICLE

Schizophrenia risk variants modulate transcription factor binding and gene expression in cortical cell types

Nathalie Gerstner[1,2,3] · Anna S. Fröhlich[1,2] · Natalie Matosin[4] · Elisabeth B. Binder[1,5] · Janine Knauer-Arloth[1,3]

Received: 9 July 2025 / Revised: 9 February 2026 / Accepted: 4 March 2026

Abstract

Schizophrenia is a complex neuropsychiatric disorder with a strong genetic component. Genome-wide association studies (GWAS) have identified numerous risk variants, but their functional impact on gene regulation remains largely unknown. A major challenge lies in interpreting the function of non-coding variants, which comprise the majority of GWAS hits, making it difficult to determine their functional consequences, particularly in identifying the target genes and cell types involved. We investigated the disruption and enhancement of transcription factor (TF) binding motifs by schizophrenia-associated GWAS SNPs in 15 cortical cell types of the human brain. We integrated single-nucleus ATAC-seq and RNA-seq data from 71 donors (36 affected by schizophrenia) with GWAS summary statistics to identify TF motifs whose binding affinities are altered by schizophrenia-associated SNPs. We found that risk alleles of schizophrenia-associated SNPs disrupt and enhance TF binding. Furthermore, we demonstrated that disrupted TF motifs can lead to altered expression of target genes, including *NAGA* in excitatory neurons and *SNX19* in protoplasmic astrocytes. These genes have been previously implicated in schizophrenia and our study provides a mechanism for their dysregulation through altered TF binding. Our findings highlight the importance of considering cell type-specific effects and provide a genome-wide map of TF motif disruptions in schizophrenia, offering insights into the regulatory mechanisms underlying disease risk. These findings may inform the development of novel therapeutic strategies targeting specific regulatory mechanisms.

Keywords Transcription factor binding · Motif alterations · Schizophrenia · Genetic variants · Cell type · Orbitofrontal cortex

Introduction

The field of schizophrenia genetics has made significant progress in recent years, with genome-wide association studies (GWAS) playing a central role in these advancements. For example, the latest GWAS on schizophrenia by Trubetskoy et al. [1] identified significant associations with schizophrenia in 287 loci, implicating a substantial polygenic contribution to disease risk. However, a major challenge in interpreting these findings lies in the fact that the majority of identified variants are located within non-coding regions of the genome, making it difficult to determine their functional consequences, particularly which genes are affected and in which cell types these schizophrenia-associated SNPs exert their effects on gene regulatory mechanisms.

These non-coding regions harbor crucial regulatory elements, such as enhancers and promoters, which influence the expression of genes [2]. Within these regulatory elements, short DNA sequences called motifs serve as binding sites for transcription factors (TFs), proteins that regulate gene expression [3]. Disruption of these motifs can alter TF binding, leading to perturbations in gene regulatory networks and potentially contributing to disease pathogenesis [4].

✉ Janine Knauer-Arloth
arloth@psych.mpg.de

1 Max Planck Institute of Psychiatry, Department Genes and Environment, Munich, Germany

2 International Max Planck Research School for Translational Psychiatry, Munich, Germany

3 Institute of Computational Biology, Helmholtz Zentrum München, Neuherberg, Germany

4 Charles Perkins Centre, The University of Sydney, Sydney, Australia

5 Department of Psychiatry and Behavioral Sciences, Emory University School of Medicine, Atlanta, USA

Published online: 21 March 2026

Previous studies, such as one by Huo et al. [5], analyzed TF binding disruption by GWAS-derived SNPs in bulk tissue samples from different regions within the human brain. However, these investigations lacked the resolution to assess the influence of schizophrenia-associated GWAS SNPs on TF motifs at the cell type-specific level. Moreover, bulk tissue analyses may not accurately reflect the regulatory landscape of specific cell types involved in schizophrenia pathogenesis. Recent advances in single-cell sequencing technologies now allow for the investigation of gene regulation with unprecedented cell type-specific resolution. This is particularly crucial in the context of brain disorders like schizophrenia, where the interplay of diverse neuronal and glial cell types is critical for healthy function.

Given that accessible and active TF motifs can vary considerably between different cell types in the brain, it is crucial to investigate the impact of schizophrenia risk variants at the single-cell level, as demonstrated by similar approaches in Parkinson's disease research [6]. Here, we focus on the orbitofrontal cortex (OFC), a brain region implicated in higher-order cognitive functions and emotional processing [7]. The human OFC, with its unique structural and functional properties not fully captured in rodent models, exhibits abnormalities in schizophrenia, including reduced gray matter volume in Brodmann area 11 [8]. This underscores the importance of studying this region directly in humans. We present a novel approach that integrates single-nucleus ATAC-seq and RNA-seq data from the OFC of a cohort comprising individuals with schizophrenia ($n=35$) and neurotypical controls ($n=36$) with the latest schizophrenia GWAS summary statistics. This strategy allowed us to identify cell type-specific TF motifs disrupted or enhanced by schizophrenia-associated GWAS SNPs. For instance, we found that schizophrenia risk variants disrupt and enhance TF binding, with a similar number of instances of increased and decreased binding affinity. Exploration of whether the gene expression of target genes was associated with these TF binding sites, revealed differential patterns between carriers and non-carriers of the alternate allele. Notably, these variants are predicted to affect the binding of several transcription factors, including EGR4. This study contributes to a deeper understanding of the genetic basis of schizophrenia and provides novel insights that may inform future research directions.

Table 1 Postmortem brain cohort summarized information: Data are presented as the mean ± SD. female (F), male (M), post-mortem interval (PMI) and RNA Integrity Number (RIN)

	Controls ($n=35$)	Cases ($n=36$)	Overall ($n=71$)
Age [years]	55.83 ± 13.56	54.81 ± 12.84	55.31 ± 13.12
Sex	13 F | 22 M	11 F | 25 M	24 F | 47 M
PMI [h]	31.80 ± 11.30	33.71 ± 16.43	32.77 ± 14.07
pH	6.66 ± 0.24	6.53 ± 0.18	6.60 ± 0.22
RIN	7.17 ± 1.34	7.32 ± 1.00	7.24 ± 1.17

Materials and methods

Postmortem brain cohort description

A detailed description of the postmortem brain cohort and tissue can be found in [9, 10]. Fresh frozen postmortem tissues of the orbitofrontal cortex (Brodmann Area 11) were obtained from the NSW Brain Tissue Resource Centre in Sydney, Australia. The cohort comprised 71 donors, including 35 neurotypical controls with no history of neurological or neuropsychiatric disorder or obvious postmortem brain pathology and 36 individuals diagnosed with schizophrenia. Groups were matched by brain pH (mean ± s.d. = 6.60 ± 0.22), postmortem interval (mean ± s.d. = 32.77 ± 14.07), age (mean ± s.d. = 55.31 ± 13.12), and sex (34% female representation), see Table 1.

DNA extraction, SNP genotyping and imputation

As described previously [9, 10], genomic DNA was isolated from 10 mg of brain tissue using the QIAamp DNA mini kit (Qiagen) and concentrated with the DNA Clean & Concentrator-5 (Zymo Research). Samples were genotyped using Illumina GSA-24v2-0_A1 arrays (Illumina Inc., San Diego, CA, USA). Quality control in PLINK v1.90b3.30 [11] included removing donors with > 2% missing data, cryptic relatives (PI-HAT > 0.125), autosomal heterozygosity deviation (|Fhet| > 4 SD), and genetic outliers (distance from mean ancestry components > 4 SD). Variants with < 98% call rate, minor allele frequency (MAF) < 1%, or Hardy–Weinberg equilibrium (HWE) p-value $\leq 10^{-6}$ were excluded. Imputation was performed using IMPUTE2 [12], following phasing in SHAPEIT, using the 1000 Genomes Phase III reference sample. Imputed SNPs with INFO score < 0.6, MAF < 5%, or HWE p-value $< 1 \times 10^{-5}$ were excluded, resulting in 6,617,712 SNPs in 71 donors.

Schizophrenia Genome-wide association study (GWAS) summary statistics

GWAS summary statistics for schizophrenia were obtained from the Psychiatric Genomics Consortium [1], based on cohorts of European ancestry, thereby matching the ethnicity of the postmortem brain cohort. All variants with a GWAS p-value $\leq 5 \times 10^{-8}$ ($n=20{,}066$ SNPs distributed across 287 loci), regardless of their linkage disequilibrium, were tested for disruption of transcription factor binding motifs. This comprehensive inclusion aimed to capture the full spectrum

of potential regulatory perturbations within GWAS-significant loci, rather than strictly pinpointing causal variants within LD blocks. The genomic coordinates of these variants were mapped to the GRCh38 genome assembly based on their rsIDs using the biomaRt package (v2.56.1) [1, 13]. Variants exhibiting negative effect sizes were recoded such that the alternative allele consistently denotes risk-increasing effects for schizophrenia rather than protective effects.

Single-nucleus (sn) sequencing

Data pre-processing

A detailed description of nuclei isolation and sequencing details, as well as the data pre-processing of the single-nucleus (sn) RNA-seq and ATAC-seq data can be found in [9, 10]. Briefly, we processed snRNA-seq data by aligning reads to a pre-mRNA reference (GRCh38, Ensembl 98) and counting UMIs with Cell Ranger (cellranger count v6.0.1) [14]. To normalize sequencing depth differences, reads were downsampled to the 75% quantile using DropletUtils (v1.12.2) [15]. We combined count matrices of all donors using Scanpy (v1.7.1) [16] and filtered nuclei (counts < 500, genes < 300, mitochondrial % ≥ 15), removing genes expressed in fewer than 500 nuclei. Doublet removal was performed [17], and data was normalized and log-transformed using sctransform (v0.3.2) [18]. Dimensionality reduction and clustering was performed, and the final dataset comprises 636,514 nuclei from 69 donors (33 unaffected, 36 affected by schizophrenia). We processed snATAC-seq data by aligning reads to a reference (GRCh38, Ensembl 98) and generating count matrices with Cell Ranger ATAC (cellranger-atac count v2.0.0) [19]. Quality control using the R package v1.0.2 ArchR [20] excluded nuclei with a TSS enrichment score < 4 and those with < 1,000 or > 100,000 unique nuclear fragments. Doublets were removed and dimensionality was reduced using iterative LSI, followed by UMAP for visualization and clustering with Seurat's FindClusters method (v4.0.4) [21]. Final filtering resulted in 319,642 nuclei from 71 donors (35 unaffected, 36 affected by schizophrenia).

As previously described, cell types were assigned to the nuclei in the snRNA-seq data through a combination of label transfer from a publicly available cortical dataset with scArches v0.4.0 [22]/scANVI [23] and manual curation of marker genes. Cluster identities in the snATAC-seq data were initially assigned by integrating it with snRNA-seq data using ArchR and Seurat's FindTransferAnchors function, labeling each snATAC-seq nucleus with the cell type of the most similar snRNA-seq nucleus. Cluster identities were then manually refined based on manual curation of marker gene scores.

Pseudobulk replicates and peak calling

To enable downstream analyses requiring replicates, we created pseudobulk replicates by summing gene expression and chromatin accessibility counts from each cell type-donor pair. This was done using an ArchR method that summarizes data from multiple similar donors within a cell type to circumvent sparsity [20].

Peak calling on snATAC-seq data was performed per cell type on pseudobulk replicates using MACS2 [24] in ArchR. The resulting peaks were merged across pseudobulk replicates and cell types into a single set ($n_{peaks} = 767{,}529$).

Marker peak identification

Marker peaks that are uniquely accessible in a specific cell type were identified with ArchR. Peaks with a $\log_2$ fold change ≥ 1 and an FDR ≤ 0.05 were defined as marker peaks (Table S1).

Transcription factor motif enrichment and filtering

Human transcription factor binding motifs ($n = 633$) were obtained from the JASPAR 2020 database [25]. We used the motifmatchr R package (v1.12.0) to determine motif presence in each peak identified during peak calling. A hypergeometric test was applied to test for enrichment of the annotated motifs in cell type-specific marker peaks. Motifs showing a binding enrichment with a significance level of $P < 1 \times 10^{-10}$ were selected (Table S2–3). We then used the chromVAR package (v1.12.0) [26] to identify highly active motifs per cell type by determining the accessibility of motif-containing peaks compared to a random background set of peaks in a bias-corrected manner (Table S4–5). Finally, we required that the gene encoding the respective TF be expressed in at least 5% of the cells of the respective cell type. For motifs belonging to heterodimers or heterotrimers, all two/three genes were required to be expressed in at least 5% of the cells (Table S6–7).

Definition of regulatory elements

For each cell type, we defined a set of single-cell candidate cis-regulatory elements (scCREs—following ENCODE convention [27]). These scCREs had to fulfill at least one of two criteria: 1) they were called as peaks in the pseudobulk samples generated for this specific cell type; 2) they are accessible in at least 5% of the individual cells within this cell type. The reasoning behind this is that peaks identified in the pseudobulk sample of one cell type can also be accessible in other cell types.

Generation of synthetic reference genome

Two synthetic reference genomes were generated with the GATK FastaAlternateReferenceMaker (v4.5.0.0) [28], one comprising schizophrenia risk alleles and the other comprising the non-risk alleles of GWAS SNPs following recoding based on effect sizes. Fasta sequences of the SNP containing scCREs were extracted with the bedtools getfasta method (v2.31.1) [29].

Differential transcription factor binding score analysis

Transcription factor binding scores were calculated per cell type on the reference and alternate sequences of SNP-containing scCREs for the TF binding motifs enriched, accessible, and expressed in the respective cell type (Table S7). We used FIMO from the MEME suite (v5.5.5) [30] with an output threshold of 0.99 to account for all possible motif hits and calculated differential binding scores GWAS SNP-containing motifs. The sum of $-\log_{10}(p\text{-values})$ of all motif hits within each SNP-containing peak determines the overall binding score of each of these peaks for both the reference and the alternate SNP sequence. Peaks without any motif hits were assigned a binding score of 0. The differential binding score of each peak is defined by the difference between the reference binding score and the alternate binding score. Differential binding within an scCRE is defined by an absolute differential binding score >3. A positive differential binding score indicates gained TF binding through the alternative allele compared to the reference allele, while a negative differential binding score indicates lost TF binding. Motifs with a difference in the number of scCREs with gained and lost TF binding ≥ 5 were defined as consistently disrupted or enhanced in the respective cell type. Thresholds are based on the distribution of differential binding scores and the difference between scCREs with gained and lost TF binding.

Mapping of SNPs to target genes

We used PLINK (v2.00a6LM) [31] to extract genotype information in the bed-format for the SNPs disrupting or enhancing TF binding. These SNPs were mapped to their putative target genes with H-MAGMA (v1.08) [32], partially incorporating cell type-specific Hi-C annotations. Specifically, we used a Hi-C mapping from cortical neurons [33] for neuronal cell types, a mapping from iPSC-derived astrocytes [34] for all astrocytes, and a mapping based on the adult dorsolateral prefrontal cortex [35] for the remaining cell types (Table S11).

Fig. 1 Workflow and data overview for identifying schizophrenia-associated SNPs affecting TF binding and gene expression. (**a**) Schematic of the study design. We analyzed single-nucleus ATAC-seq and RNA-seq data from the orbitofrontal cortex of a postmortem brain cohort comprising 35 unaffected and 36 affected by schizophrenia. These data were integrated with schizophrenia GWAS summary statistics and a TF motif database (Jaspar 2020) to identify SNPs that disrupt or enhance TF binding. Differential gene expression analysis was performed to assess the impact of these SNPs on target gene expression. (**b**) UMAP visualizations of the snATAC-seq (right) and snRNA-seq (left) data, colored by cell type. (**c**) Manhattan plot of the 20,066 schizophrenia GWAS genome-wide significant hits ($P \leq 5 \times 10^{-8}$). The x-axis shows genomic coordinates, and the y-axis shows the GWAS effect size (beta) with beta >0 indicating risk SNPs and beta <0 protective SNPs. The color intensity of the points represents the $-\log_{10}(P\text{-value})$

Differential gene expression analysis

Differential gene expression analysis of target genes between alternate allele (risk or protective) carriers and non-carriers was performed with DESeq2 (v1.30.1) [36] on a pseudobulk level. Only target genes with at least 10 counts in at least 75% of the pseudobulk samples were included in the analysis. Case/control status, sex, age, brain pH, RNA integrity number (RIN), and postmortem interval (PMI) were included as covariates in the model. Target genes with an FDR ≤ 0.1 were defined as significantly differentially expressed. For visualization, the count data were transformed with the voom method and corrected for sex, age, brain pH, RIN, and PMI using the removeBatchEffect function from the limma package (v3.46.0) [37]. Note that the target genes of some disrupted and enhanced TF binding sites could not be tested due to missing genotype information or too few carriers or non-carriers of the alternate allele (Table S12).

Results

In this study, we employed a multi-step workflow to investigate the disruptions and enhancements of transcription factor (TF) motifs by schizophrenia-associated GWAS SNPs in 15 cell types of the orbitofrontal cortex that we briefly summarize below and in Fig. 1a. First, we identified marker peaks for each cell type based on single-nucleus ATAC-seq data from postmortem orbitofrontal cortex tissue ($n=71$ individuals, 36 affected by schizophrenia, 35 neurotypical controls), whereby the number of marker peaks identified varied across cell types (see Table S1). Within these peaks, we determined the enrichment of TF motifs (see Table S2−3). A further filtering step narrowed the motifs down to those that are highly accessible (see Table S4−5). This step also required that the gene encoding the TF be expressed in more than 5% of the nuclei of the respective cell type (see Table S6−7).

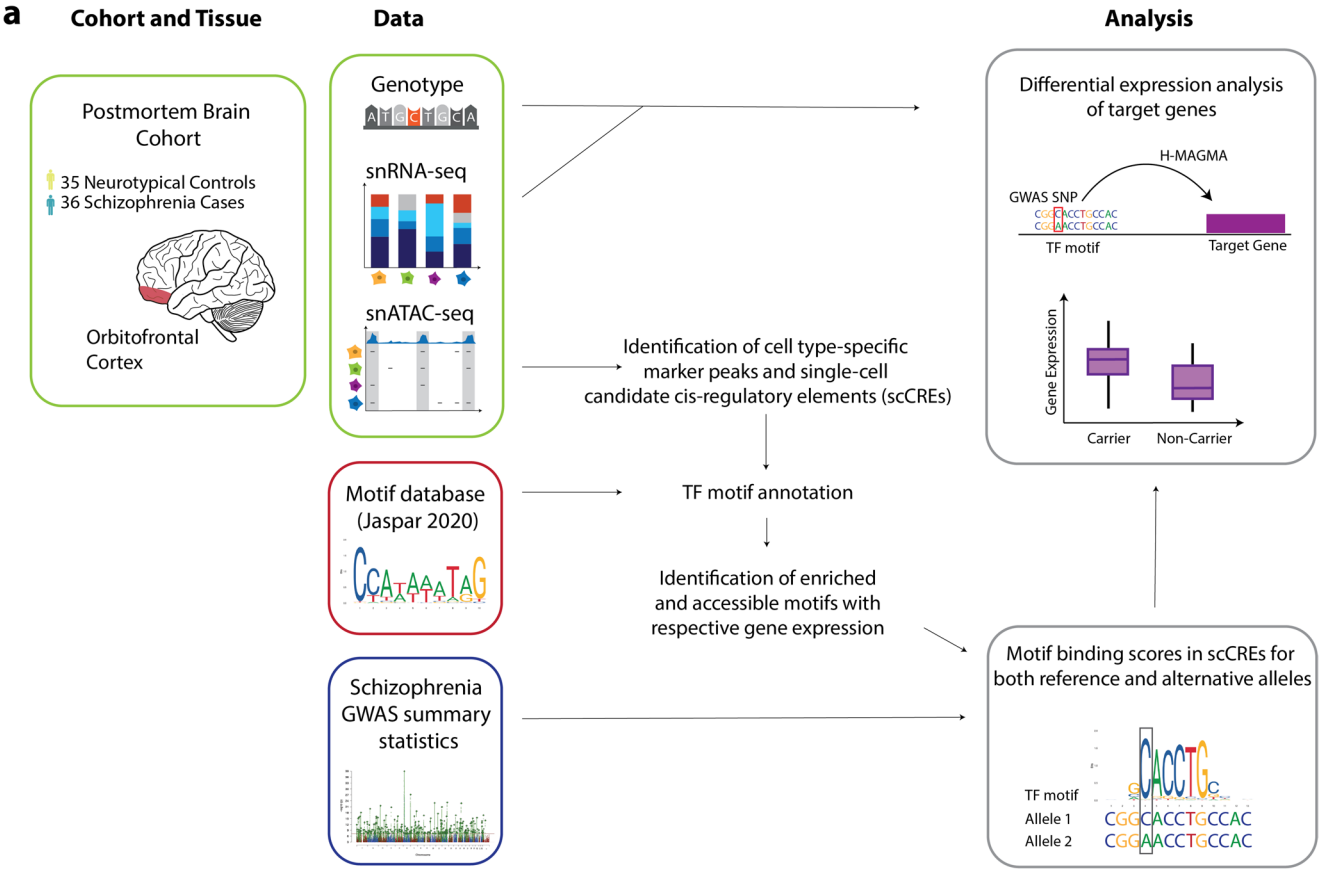
a
Cohort and Tissue
Data
Analysis
Postmortem Brain Cohort
35 Neurotypical Controls
36 Schizophrenia Cases
Orbitofrontal Cortex
Genotype
snRNA-seq
snATAC-seq
Motif database (Jaspar 2020)
Schizophrenia GWAS summary statistics
Identification of cell type-specific marker peaks and single-cell candidate cis-regulatory elements (scCREs)
TF motif annotation
Identification of enriched and accessible motifs with respective gene expression
Differential expression analysis of target genes
H-MAGMA
GWAS SNP
TF motif
Target Gene
Gene Expression
Carrier
Non-Carrier
Motif binding scores in scCREs for both reference and alternative alleles
TF motif
Allele 1
Allele 2

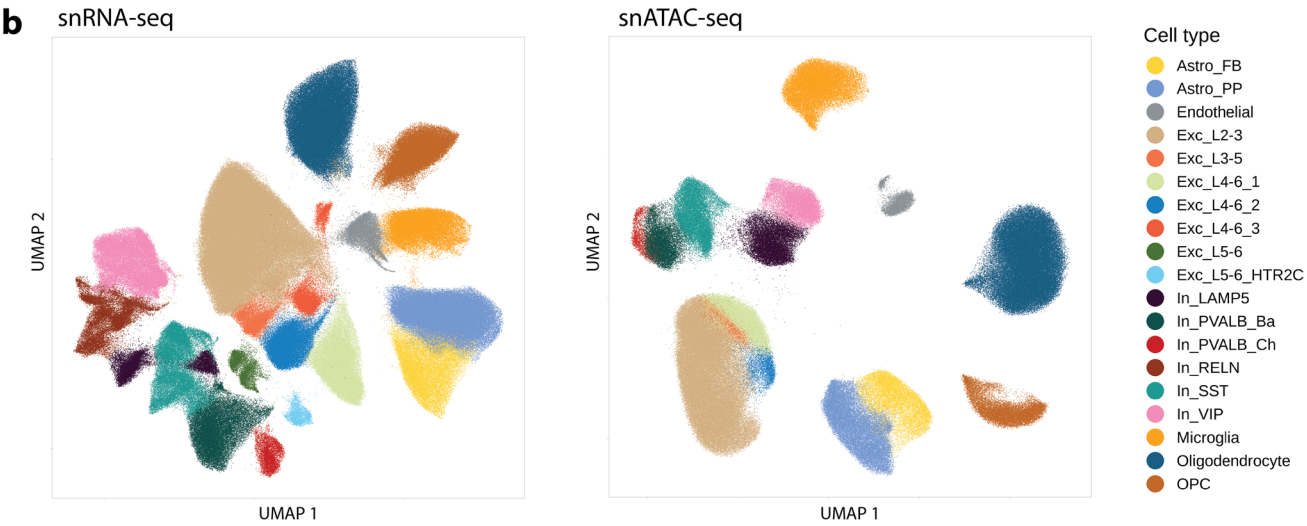
b
snRNA-seq
snATAC-seq
UMAP 1
UMAP 2
Cell type
Astro_FB
Astro_PP
Endothelial
Exc_L2-3
Exc_L3-5
Exc_L4-6_1
Exc_L4-6_2
Exc_L4-6_3
Exc_L5-6
Exc_L5-6_HTR2C
In_LAMP5
In_PVALB_Ba
In_PVALB_Ch
In_RELN
In_SST
In_VIP
Microglia
Oligodendrocyte
OPC

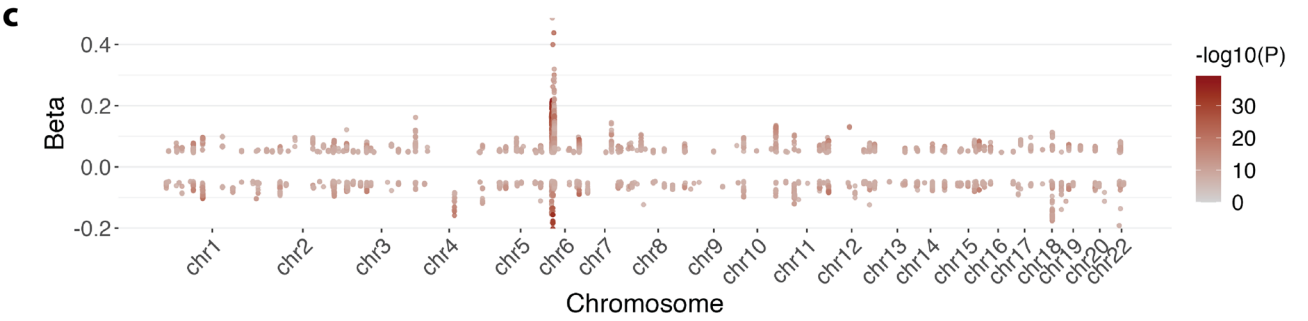
c
Beta
0.4
0.2
0.0
-0.2
-log10(P)
30
20
10
0
chr1
chr2
chr3
chr4
chr5
chr6
chr7
chr8
chr9
chr10
chr11
chr12
chr13
chr14
chr15
chr16
chr17
chr18
chr19
chr20
chr22
Chromosome

Using the latest schizophrenia GWAS summary statistics [1], we assessed the effects of GWAS SNP risk alleles (Table S8) on TF binding. We calculated binding scores for both alleles within single-cell candidate cis-regulatory elements (scCREs, see Methods), which encompass accessible regions from multiple cell types. This approach allowed us to identify TFs with motifs that were consistently disrupted or enhanced by the presence of GWAS SNPs.

Subsequently, we examined genotype information from the postmortem brain samples, mapping individuals based on their genotypes into carriers and non-carriers of the respective risk allele. We mapped SNPs located in disrupted or enhanced motifs to putative target genes (see Methods) and we performed differential expression analysis to compare gene expression levels between carriers and non-carriers of risk alleles. This analysis provided insights into the functional consequences of motif disruptions on gene regulation in schizophrenia.

Our single-nucleus sequencing data comprised chromatin accessibility information (snATAC-seq) in 319,642 nuclei in 15 cell types and gene expression quantification (snRNA-seq) for 26,195 genes in 636,514 nuclei in 19 cell types (Fig. 1b). The schizophrenia GWAS data utilized in our analysis comprised 20,066 genome-wide significant hits ($P \leq 5 \times 10^{-8}$) that were mapped to the GRCh38 genome assembly, including 13,755 risk (GWAS beta > 0) and 6,311 protective SNPs (GWAS beta < 0) (Fig. 1c). This robust dataset enabled us to systematically explore the intricate relationships between genetic variants, TF motif disruptions, and gene expression changes in the context of genetic risk for schizophrenia.

Cell type-specific enrichment of transcription factor motifs

We were interested in TFs particularly active in the transcriptional regulation of specific cell types, as cell type-specific TF activity can reveal unique regulatory mechanisms and highlight differential susceptibility to schizophrenia risk variants. Therefore, we identified motifs enriched in cell type-specific accessible chromatin that are also active and exhibit corresponding transcription of the TF-expressing gene. First, we identified cell type-specific marker peaks uniquely accessible in each cell type (Fig. 2a). The number of marker peaks per cell type ranges from 2,022 in endothelial cells to 29,613 in excitatory neurons of layers 2 to 3 (Supp. Figure 1a). We annotated human TF binding motifs from JASPAR 2020 within these marker peaks and tested for enrichment compared to background regions (Fig. 2a). These enrichments were similar among sub-cell types within major groups (excitatory neurons, inhibitory neurons, and glial cells) and also showed some overlap between major groups, such as Kruppel-like factors enriched in excitatory neurons and glial cells (Fig. 2b). The number of enriched motifs varied from 57 in LAMP5 interneurons to 153 in microglia (Fig. 2c). Because a substantial proportion of schizophrenia-associated GWAS SNPs are located within the MHC and microglia have a prominent immune component, we repeated the analysis excluding all genome-wide significant SNPs within the extended MHC region (Chr6:26 Mb-34 Mb). The number of enriched motifs in microglia decreased only minimally from 153 to 151, indicating that there is no inflation of MHC-driven associations in our target analysis.

For downstream analysis of motif disruption, we further filtered these motifs by determining their accessibility deviation (a measure of motif accessibility compared to a random background; see Methods), narrowing the set to highly accessible and active motifs. This results in the number of motifs now ranging from 8 in LAMP5 interneurons to 65 in excitatory neurons of layers 2 to 3 (Fig. 2c). The final filtering step, retaining only motifs of TFs with the respective gene expressed in at least 5% of the nuclei, resulted in a set of motifs per cell type ranging from 1 in VIP interneurons and 24 in excitatory neurons of layers 2 to 3 (Fig. 2c).

Finally, we defined scCREs in each cell type for downstream analysis which were then tested for binding disruptions and enhancements (see Methods). The number of scCREs per cell type ranges from 47,673 in excitatory neurons of layer 4 to 6, cluster 2 to 106,435 in endothelial cells (Supp. Figure 1b).

Differential transcription factor binding analysis reveals disrupted motifs in schizophrenia

We tested the set of enriched and active motifs with respective gene expression in each cell type for motif disruption or enhancement through the risk allele of schizophrenia-related GWAS SNPs (Fig. 3a, Table S8). The analysis of differential binding scores revealed that GWAS variants in scCREs both disrupt and enhance TF binding. Specifically, 20 out of 126 tested motifs showed a consistent reduction in TF binding affinity due to risk GWAS-alleles, compared to 15 motifs that exhibited a consistently increased binding affinity (Fig. 3b, Table S10). Notably, NFIB (in fibrous (FB) and protoplasmic (PP) astrocyte subtypes), NFIX, EMX2 and RORB (in protoplasmic astrocyte subtypes), NR2F1 (in endothelial cells), EGR4, MGA and MAFK (in excitatory neurons of layers 2/3), ELK4, ELF1, ELF2, USF2, ETV6, ETS2, IRF8, IRF3, and CEBPD (in microglia), and SOX2 and SOX8 (in oligodendrocytes) were associated with risk GWAS-allele-induced binding disruptions, while NFIX (in fibrous astrocytes and oligodendrocyte precursor cells), SP4, KLF3 and KLF6 (in endothelial cells), JUNB

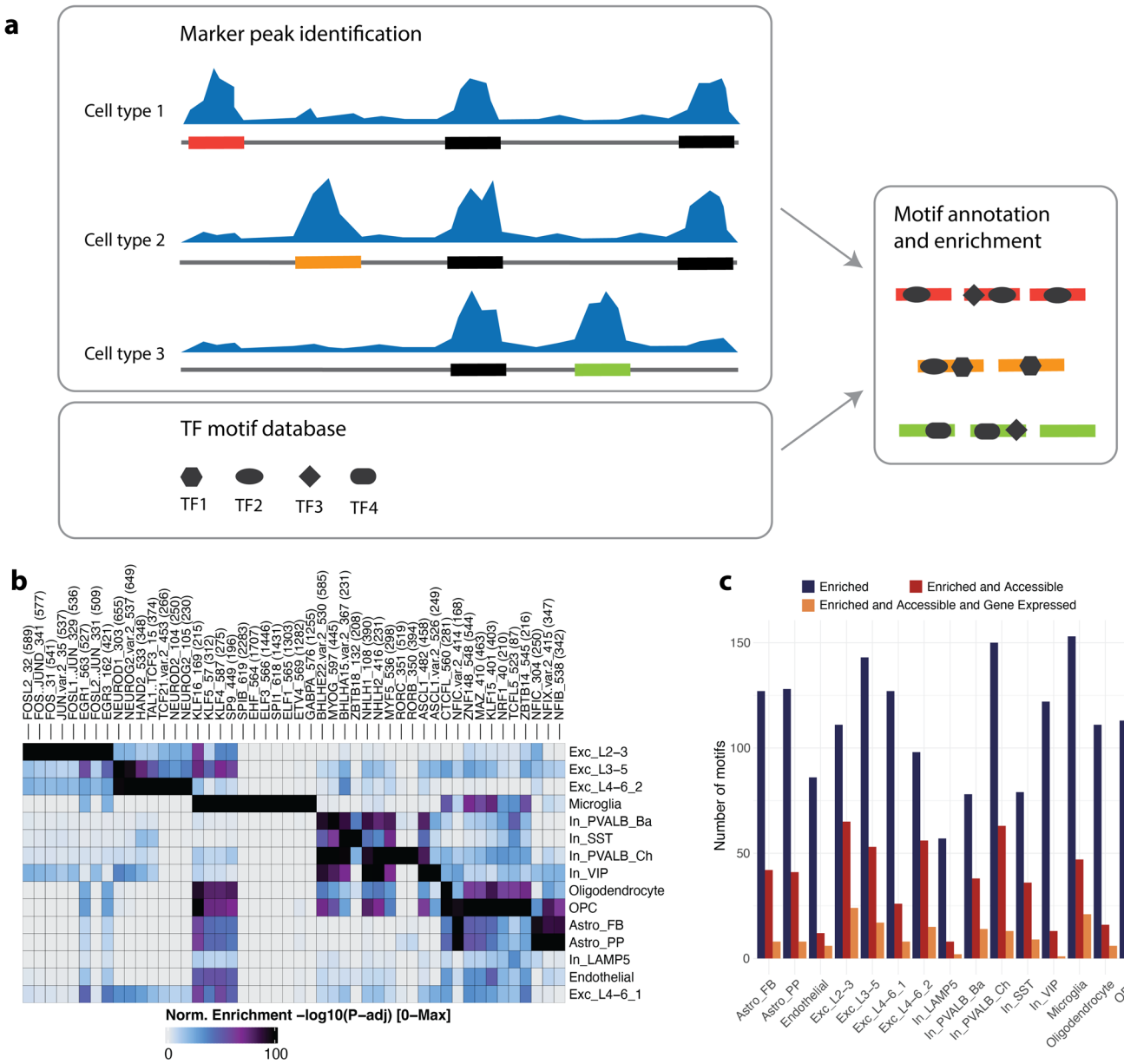

Fig. 2 Identification of cell type-specific TF motifs in the human orbitofrontal cortex. (**a**) Schematic overview of the workflow for identifying cell type-specific TF motifs. First, marker peaks are identified for each cell type based on single-nucleus ATAC-seq data. Then, TF motifs from the Jaspar database are annotated within these peaks and tested for enrichment. Different shapes indicate distinct TF motifs, and the color code represents scCREs. (**b**) Heatmap showing the enrichment of TF motifs across different cell types. The color scale indicates the -$\log_{10}$(FDR) of the enrichment test. Higher values represent greater enrichment. (**c**) Bar plot showing the number of enriched TF motifs in each cell type. The red bars represent the number of motifs passing the enrichment threshold ($\log_2$FC ≥ 1 and FDR ≤ 0.05), while the blue bars represent the number of motifs passing both the enrichment threshold and the accessibility filter (chromVAR deviation)

and FOSL2-JUN complex (in excitatory neurons of layers 2/3), MAFG, MEF2D, JDP2, CREB1 (in different subtypes of inhibitory neurons) and SPI1 and RUNX2 (in microglia) were associated with risk GWAS-allele-induced binding enhancement. Generally, motifs across the genome exhibit disruptions in both directions, with changes in binding affinity rarely being consistently towards either gain or loss (Supp. Figure 2).

Disrupted transcription factor motifs lead to differential gene expression in schizophrenia

To examine the transcriptional effects of GWAS SNPs on the consistently disrupted and enhanced motifs, we tested for differential expression between carriers and non-carriers of risk alleles (Fig. 4a). First, we collected genotype information from each donor in our postmortem brain cohort

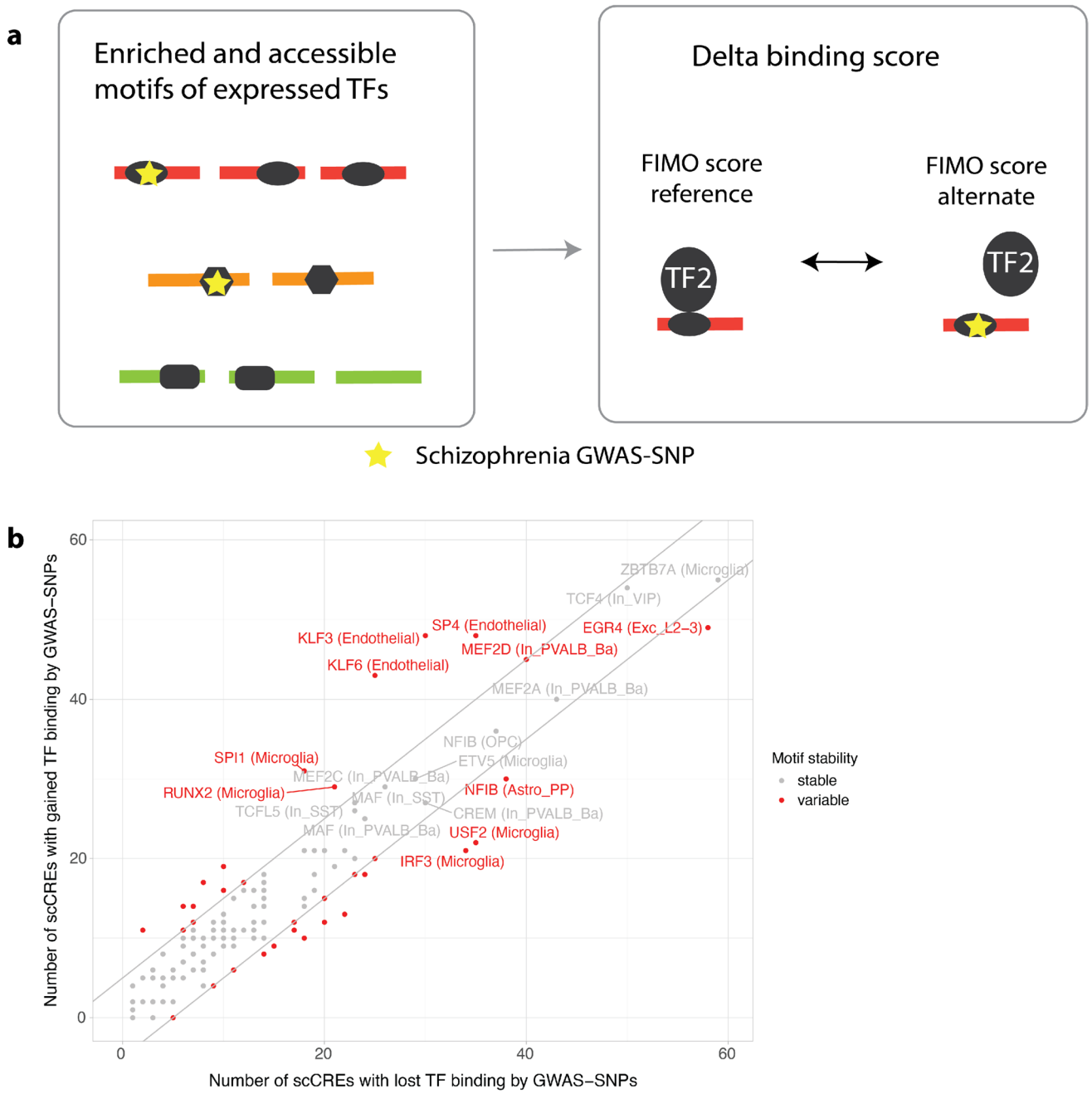

Fig. 3 Differential TF binding analysis. (**a**) Schematic overview of the differential TF binding analysis. Enriched and accessible motifs of expressed TFs are tested for disruption or enhancement by schizophrenia-associated SNPs (yellow star). TF binding scores are calculated for both the risk and non-risk alleles of SNPs located within scCREs. The delta binding score represents the difference between these scores. (**b**) Scatter Plot showing the number of scCREs with gained TF binding versus the number of scCREs with lost TF binding for schizophrenia-associated GWAS SNPs. Each dot represents a TF motif in a specific cell type. Red dots indicate motifs with a significant difference (≥ 5) in the number of scCREs with gained versus lost TF binding, suggesting consistent disruption or enhancement

matching with schizophrenia GWAS SNPs. The overall number of risk alleles is slightly higher in donors affected by schizophrenia compared to those unaffected (Fig. 4b). We next used H-MAGMA [32] to identify the putative target genes of the disrupting or enhancing variants (Table S11). The number of SNPs that could be mapped to a target gene ranged from 2 to 96 per motif, and the number of genes they were mapped to ranged from 6 to 69 for risk variants (Fig. 4c). We observed 24 combinations of significant differential expression (FDR$\leq$0.1) of target genes and respective alteration of TF binding motifs by risk alleles of GWAS SNPs, suggesting a functional impact of these SNPs on gene

regulation (Table S13). For instance, in excitatory neurons of layer 2 to 3 (Exc_L2-3), the risk allele of SNP rs133376 on chromosome 22 (also rs133377 and rs2859438) alters an accessible binding motif of EGR4, and the respective target gene *NAGA* exhibits differential expression between carriers and non-carriers of the risk allele (FC = 0.43, FDR = 0.003, Fig. 4e). Similarly, in protoplasmic astrocytes (Astro_PP), the risk allele of SNP rs3751033 on chromosome 11 alters an accessible binding motif of NFIB, and the respective target gene *SNX19* exhibits differential expression between carriers and non-carriers of the risk allele (FC = 0.38, FDR = 0.01, Fig. 4f).

Discussion

This study presents a comprehensive analysis of how schizophrenia-associated genetic variants disrupt or enhance TF binding sites or TF motifs in different types of brain cells. Our analysis revealed that the number of TF binding sites affected by schizophrenia-associated SNPs and located within accessible chromatin regions varies considerably across cell types, with microglia being the cell type exhibiting the highest number. Microglia, the primary immune cells in the brain, are highly implicated in schizophrenia pathophysiology [38, 39]. In our sample, microglia had the highest number of enriched TF motifs. Importantly, this enrichment remained robust even after exclusion of the extended MHC locus indicating that the observed signal is not driven solely by MHC-associated variants. When considering accessibility and gene expression, excitatory neurons of layers 2 to 3 emerged as a critical cell type. However, this finding may be linked to power differences between cell types, as highlighted in a previous paper based on the dataset [10]. These neurons play a crucial role in maintaining healthy cortical processes [40] and their dysfunction has been implicated in schizophrenia [41]. Our study provides a valuable resource by pinpointing specific TFs and their target genes in these neurons in schizophrenia.

Furthermore, by including GWAS SNPs in our analysis, we identified that the alteration of TF binding motifs by schizophrenia risk alleles disrupts and enhances binding (15.9% disrupted vs. 11.9% enhanced—20 and 15 out of 126). The observation that risk alleles enhance TF binding motifs nearly as frequently as they disrupt them suggests a complex regulatory landscape. Such a balanced effect highlights the intricate and likely compensatory nature of gene regulation in complex disorders. These observations suggest that schizophrenia genetic risk may be partly mediated by the disruption of crucial regulatory molecular pathways, contributing to altered gene expression patterns in specific cortical neurons. By integrating single-nucleus sequencing data with GWAS summary statistics, we provide valuable insights into the regulatory mechanisms underlying schizophrenia risk, linking genetic variation to altered TF binding and downstream gene expression changes.

Importantly, we identified several instances where altered TF motifs were associated with expression levels of target genes. For example, in excitatory neurons of layer 2 to 3, we show that the schizophrenia GWAS SNP rs133376 disrupts the Early Growth Response 4 (EGR4) binding motif. This alteration is associated with an increase in *alpha-N-acetylgalactosaminidase* (*NAGA*) expression, suggesting that EGR4 acts as a negative regulator of NAGA in these neurons, and that the risk allele impairs this regulatory mechanism. This finding is particularly interesting given previous evidence implicating *NAGA* in schizophrenia [42] and its role in glycosylation, a process which is crucial for neuronal development and synaptic plasticity [43]. Alterations in glycan structures on proteins that are critical for synaptic function contribute to the cognitive deficits observed in schizophrenia patients. Other studies have identified genetic variants affecting glycosylation pathways, including potential influences from *NAGA*-related genes [44]. Recent research suggests *NAGA* regulates dendritic spine density, further supporting the hypothesis of dendritic spine pathology in schizophrenia [45]. Our study adds to this knowledge by providing a potential mechanism for *NAGA* dysregulation through the alteration of EGR4 binding, a TF also known to be involved in neuronal development and synaptic plasticity [46]. This suggests a potential interplay between EGR4, *NAGA*, glycosylation, and dendritic spine function in schizophrenia. Further investigation into these complex interactions is warranted and may pave the way for novel therapeutic approaches.

We also observed that the SNP rs3751033 modulates a Nuclear factor 1 B-type (NFIB) binding motif in protoplasmic astrocytes, coinciding with increased expression of *sorting nexin 19* (*SNX19*), a gene located at a well-established schizophrenia risk locus. NFIB is a transcription factor with a recognized role in brain and cortical development, as well as in the differentiation of neural progenitor cells [47, 48]. Disruption of NFIB binding at this locus may therefore alter local regulatory activity, leading to dysregulated expression of target genes like *SNX19*. Notably, *SNX19* has been implicated in schizophrenia through GWAS and eQTL analyses, which have shown that schizophrenia risk variants are associated with altered expression of multiple *SNX19* transcript isoforms in postmortem human brain tissue [42, 49]. While the exact mechanism and direction of effect warrant further investigation, these observations suggest that altered NFIB binding could contribute to *SNX19* dysregulation in schizophrenia, consistent with previous evidence of its altered expression.

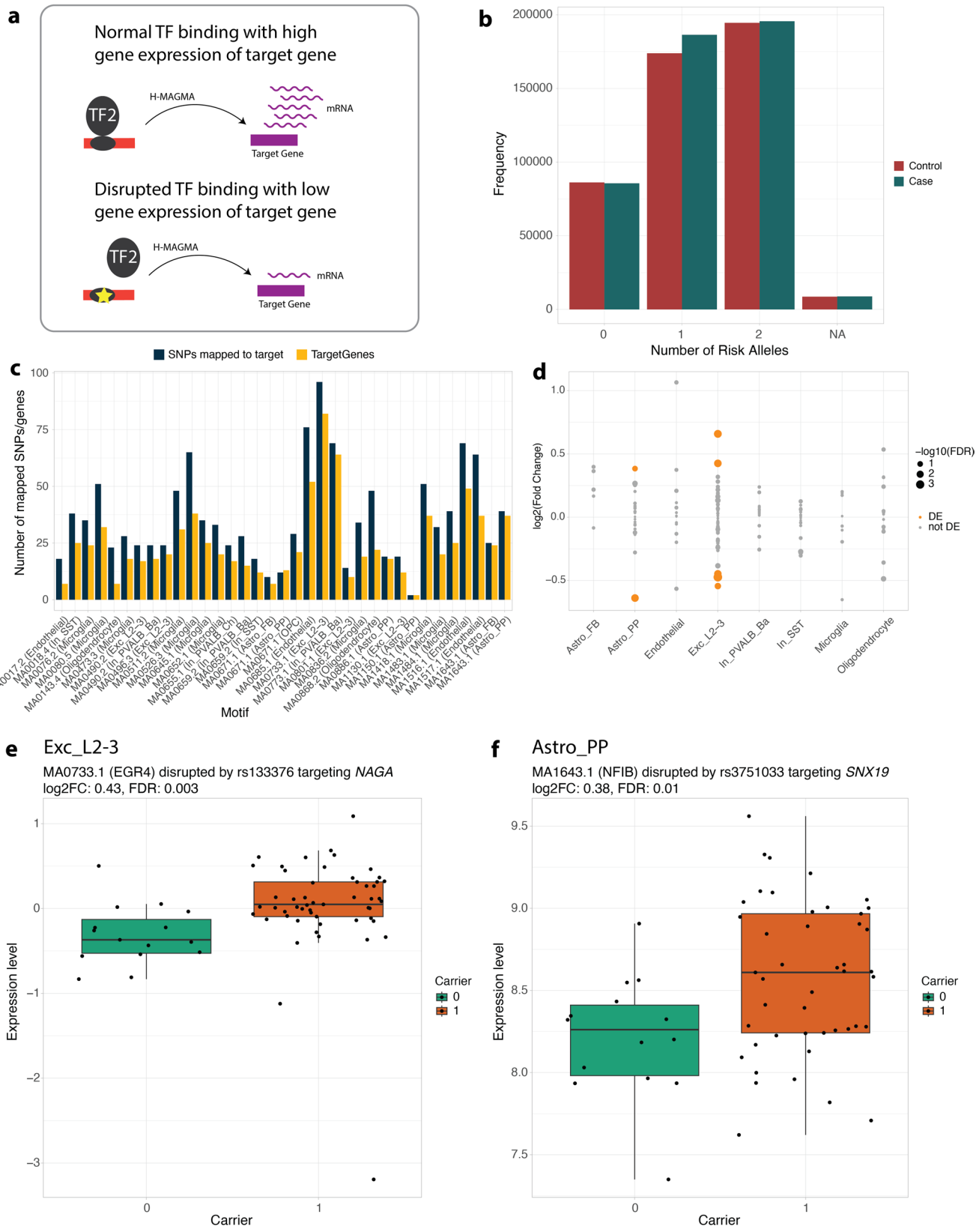
a
Normal TF binding with high gene expression of target gene
TF2
H-MAGMA
mRNA
Target Gene
Disrupted TF binding with low gene expression of target gene
TF2
H-MAGMA
mRNA
Target Gene
b
Frequency
Number of Risk Alleles
Control
Case
c
SNPs mapped to target
TargetGenes
Number of mapped SNPs/genes
Motif
d
log2(Fold Change)
–log10(FDR)
DE
not DE
Astro_FB
Astro_PP
Endothelial
Exc_L2–3
In_PVALB_Ba
In_SST
Microglia
Oligodendrocyte
e
Exc_L2-3
MA0733.1 (EGR4) disrupted by rs133376 targeting NAGA
log2FC: 0.43, FDR: 0.003
Expression level
Carrier
f
Astro_PP
MA1643.1 (NFIB) disrupted by rs3751033 targeting SNX19
log2FC: 0.38, FDR: 0.01
Expression level
Carrier

Fig. 4 Disrupted TF motifs associated with differential gene expression in schizophrenia. (**a**) Schematic illustrating the impact of disrupted TF binding on target gene expression. Normal TF binding is associated with high gene expression, while disrupted binding can lead to low gene expression. (**b**) Bar plots showing the overall number of risk alleles across the significant GWAS SNPs color coded by case/control status of the individual. (**c**) Bar plot showing the number of SNPs mapped to a target gene per TF motif. Dark blue bars represent the total number of SNPs located in a disrupted motif that could be mapped to a target gene, while yellow bars represent the number of target genes the respective SNPs are mapped to. (**d**) Dot plot showing the $-\log_{10}$(FDR) of differential gene expression analysis for target genes of schizophrenia-associated GWAS SNPs. Each dot represents a target gene in a specific cell type. Orange dots indicate significant differential expression (FDR $\leq$ 0.1). (**e–f**) Boxplots showing the expression levels of (**e**) *NAGA* in excitatory neurons of layer 2/3 and (**f**) *SNX19* in protoplasmic astrocytes, comparing carriers and non-carriers of the risk allele

Beyond the target genes, TFs themselves are also of significant interest as potential therapeutic targets for schizophrenia. Given TFs can be modulated by drugs, identifying those involved in the disease could pave the way for novel treatment strategies. By targeting specific TFs, researchers could aim to restore normal gene expression patterns and reduce schizophrenia symptoms or even prevent disease onset. This approach holds promise for personalized medicine, as different TFs may be involved in different subtypes of schizophrenia or in individuals with specific genetic backgrounds. Further investigation of TFs as therapeutic targets is warranted, with the potential to lead to more effective and personalized treatments for this complex disorder.

Our study has several limitations. The use of the JASPAR 2020 TF database restricts the analysis to a set of predefined transcription factors. Inclusion of all schizophrenia-associated SNPs offers a broad view but makes pinpointing causal variants within LD blocks challenging, which could dilute signal. Quantifying motif disruptions at the peak level offers a regional summary but does not provide statistical significance for individual motif changes, so results should be interpreted as exploratory. Experimental validation, such as ChIP-seq, is currently limited by the availability of cell-type-specific human brain tissue. Finally, our primarily European-ancestry cohort may limit the generalizability of these findings.

In conclusion, our study provides a quantitative map of TF motif disruptions and enhancements by schizophrenia-associated GWAS SNPs. By linking these genetic variants to altered TF binding and gene expression, we highlight regulatory mechanisms contributing to schizophrenia risk. Further investigation of these disrupted pathways and the implicated TFs and target genes will be crucial for advancing our understanding of schizophrenia pathogenesis and developing novel therapeutic strategies.

Supplementary Information The online version contains supplementary material available at https://doi.org/10.1007/s00018-026-06177-2.

Acknowledgements The authors thank Prof. Dr. Michael Ziller, Dr. Miriam Gagliardi, Dr. Darina Czamara, Dr. Jade Martins, Maik Ködel, Monika Rex-Haffner, Vanessa Murek, and Susann Sauer for their contributions to data generation and processing. We also thank the Medical Genomics Group, the Translational Genomics Team (Max Planck Institute of Psychiatry), the donors and their families, and the New South Wales Brain Tissue Resource Centre. Research was supported by the National Institute of Alcohol Abuse and Alcoholism (NIAAA012725-15). The content is solely the responsibility of the authors and does not represent the official views of the National Institutes of Health.

Author contributions N.G. and J.K.-A. conceptualized the study and conducted the formal analysis. N.G., A.S.F., N.M. and J.K.-A. developed the methodology. N.G. developed the software and performed the investigation and data curation. N.G. and J.K.-A. wrote the original draft. N.G., A.S.F., N.M., E.B.B., and J.K.-A. reviewed and edited the manuscript. N.G. generated the visualizations. E.B.B. and J.K.-A. supervised the study. A.S.F. and J.K.-A. handled project administration. N.M. and E.B.B. acquired funding.

Funding Open Access funding enabled and organized by Projekt DEAL. This work was supported by the Hope for Depression Research Foundation. Human brain tissue acquisition was funded by the Alexander von Humboldt Foundation research support package awarded to Dr. Natalie Matosin. Nathalie Gerstner is supported by the Joachim Herz Foundation.

Data availability The computational code developed for this study has been made available on GitHub at https://github.molgen.mpg.de/mpip/TFbinding_CorticalCells, while the preprocessed and raw single-nuclei data is available at GEO (accession number RNA: GSE254569, accession number ATAC: GSE256207).

Declarations

Ethics approval Ethics approval was obtained from both the Ludwig Maximilians-Universität (22–0523) and the Human Research Ethics Committees at the University of Wollongong (HE2018/351). Donors or their next of kin provided informed consent for brain donation.

Competing interests The authors have no relevant financial or non-financial interests to disclose.

References

1. Trubetskoy V, Pardiñas AF, Qi T et al (2022) Mapping genomic loci implicates genes and synaptic biology in schizophrenia. Nature 604:502–508
2. Zhong W, Liu W, Chen J et al (2022) Understanding the function of regulatory DNA interactions in the interpretation of non-coding GWAS variants. Front Cell Dev Biol 10:957292
3. Lis M, Walther D (2016) The orientation of transcription factor binding site motifs in gene promoter regions: does it matter? BMC Genomics 17:185
4. Spielmann M, Mundlos S (2016) Looking beyond the genes: the role of non-coding variants in human disease. Hum Mol Genet 25:R157–R165
5. Huo Y, Li S, Liu J et al (2019) Functional genomics reveal gene regulatory mechanisms underlying schizophrenia risk. Nat Commun 10:1–19
6. Lee AJ, Kim C, Park S et al (2023) Characterization of altered molecular mechanisms in Parkinson's disease through cell type–resolved multiomics analyses. Sci Adv. https://doi.org/10.1126/sciadv.abo2467
7. Jackowski AP, Araújo Filho GM et al (2012) The involvement of the orbitofrontal cortex in psychiatric disorders: an update of neuroimaging findings. Rev Bras Psiquiatr 34:207–212
8. Frisoni GB, Prestia A, Adorni A et al (2009) In vivo neuropathology of cortical changes in elderly persons with schizophrenia. Biol Psychiatry 66:578–585
9. Fröhlich AS, Gerstner N, Gagliardi M et al (2024) Single-nucleus transcriptomic profiling of human orbitofrontal cortex reveals convergent effects of aging and psychiatric disease. Nat Neurosci. https://doi.org/10.1038/s41593-024-01742-z
10. Gerstner N, Fröhlich AS, Matosin N et al (2025) Contrasting genetic predisposition and diagnosis in psychiatric disorders: a multi-omic single-nucleus analysis of the human OFC. Sci Adv 11:2290
11. Chang CC, Chow CC, Tellier LC et al (2015) Second-generation PLINK: rising to the challenge of larger and richer datasets. Gigascience 4:7
12. Howie BN, Donnelly P, Marchini J (2009) A flexible and accurate genotype imputation method for the next generation of genome-wide association studies. PLoS Genet 5:e1000529
13. Durinck S, Spellman PT, Birney E, Huber W (2009) Mapping identifiers for the integration of genomic datasets with the R/Bioconductor package biomaRt. Nat Protoc 4:1184–1191
14. Zheng GXY, Terry JM, Belgrader P et al (2017) Massively parallel digital transcriptional profiling of single cells. Nat Commun 8:14049
15. Lun ATL, Riesenfeld S, Andrews T et al (2019) EmptyDrops: distinguishing cells from empty droplets in droplet-based single-cell RNA sequencing data. Genome Biol 20:63
16. Wolf FA, Angerer P, Theis FJ (2018) SCANPY: large-scale single-cell gene expression data analysis. Genome Biol 19:15
17. Xi NM, Li JJ (2021) Protocol for executing and benchmarking eight computational doublet-detection methods in single-cell RNA sequencing data analysis. STAR Protoc. https://doi.org/10.1016/j.xpro.2021.100699
18. Hafemeister C, Satija R (2019) Normalization and variance stabilization of single-cell RNA-seq data using regularized negative binomial regression. Genome Biol 20:296
19. Satpathy AT, Granja JM, Yost KE et al (2019) Massively parallel single-cell chromatin landscapes of human immune cell development and intratumoral T cell exhaustion. Nat Biotechnol 37:925–936
20. Granja JM, Corces MR, Pierce SE et al (2021) ArchR is a scalable software package for integrative single-cell chromatin accessibility analysis. Nat Genet 53:403–411
21. Hao Y, Hao S, Andersen-Nissen E et al (2021) Integrated analysis of multimodal single-cell data. Cell 184:3573-3587.e29
22. Lotfollahi M, Naghipourfar M, Luecken MD et al (2022) Mapping single-cell data to reference atlases by transfer learning. Nat Biotechnol 40:121–130
23. Xu C, Lopez R, Mehlman E et al (2021) Probabilistic harmonization and annotation of single-cell transcriptomics data with deep generative models. Mol Syst Biol 17:e9620
24. Zhang Y, Liu T, Meyer CA et al (2008) Model-based analysis of ChIP-Seq (MACS). Genome Biol 9:R137
25. Fornes O, Castro-Mondragon JA, Khan A et al (2020) JASPAR 2020: update of the open-access database of transcription factor binding profiles. Nucleic Acids Res 48:D87–D92
26. Schep AN, Wu B, Buenrostro JD, Greenleaf WJ (2017) chromVAR: inferring transcription-factor-associated accessibility from single-cell epigenomic data. Nat Methods 14:975–978
27. Moore JE, Purcaro MJ, Pratt HE et al (2020) Expanded encyclopaedias of DNA elements in the human and mouse genomes. Nature 583:699–710
28. McKenna A, Hanna M, Banks E et al (2010) The Genome Analysis Toolkit: a MapReduce framework for analyzing next-generation DNA sequencing data. Genome Res 20:1297–1303
29. Quinlan AR, Hall IM (2010) BEDTools: a flexible suite of utilities for comparing genomic features. Bioinformatics 26:841–842
30. Cuellar-Partida G, Buske FA, McLeay RC et al (2012) Epigenetic priors for identifying active transcription factor binding sites. Bioinformatics 28:56–62
31. Purcell S, Neale B, Todd-Brown K et al (2007) PLINK: a tool set for whole-genome association and population-based linkage analyses. Am J Human Gen 81:559–575
32. Sey NYA, Hu B, Mah W et al (2020) A computational tool (H-MAGMA) for improved prediction of brain-disorder risk genes by incorporating brain chromatin interaction profiles. Nat Neurosci 23:583–593
33. Rajarajan P, Borrman T, Liao W et al (2018) Neuron-specific signatures in the chromosomal connectome associated with schizophrenia risk. Science. https://doi.org/10.1126/science.aat4311
34. Hu B, Won H, Mah W et al (2021) Neuronal and glial 3D chromatin architecture informs the cellular etiology of brain disorders. Nat Commun 12:1–13
35. Ashley-Koch AE, Crawford GE, Garrett ME et al (2018) Comprehensive functional genomic resource and integrative model for the human brain. Science. https://doi.org/10.1126/science.aat8464
36. Love MI, Huber W, Anders S (2014) Moderated estimation of fold change and dispersion for RNA-seq data with DESeq2. Genome Biol 15:550
37. Ritchie ME, Phipson B, Wu D et al (2015) limma powers differential expression analyses for RNA-sequencing and microarray studies. Nucleic Acids Res 43:e47
38. Laskaris LE, Di Biase MA, Everall I et al (2016) Microglial activation and progressive brain changes in schizophrenia. Br J Pharmacol 173:666–680
39. Zhuo C, Tian H, Song X et al (2023) Microglia and cognitive impairment in schizophrenia: translating scientific progress into novel therapeutic interventions. Schizophrenia (Heidelb) 9:42
40. Shepherd GMG, Svoboda K (2005) Laminar and columnar organization of ascending excitatory projections to layer 2/3 pyramidal neurons in rat barrel cortex. J Neurosci 25:5670–5679
41. Lewis DA, González-Burgos G (2008) Neuroplasticity of neocortical circuits in schizophrenia. Neuropsychopharmacology 33:141–165

42. Fromer M, Roussos P, Sieberts SK et al (2016) Gene expression elucidates functional impact of polygenic risk for schizophrenia. Nat Neurosci 19:1442
43. Licinio J, Wong M-L (2020) Advances in schizophrenia research: glycobiology, white matter abnormalities, and their interactions. Mol Psychiatry 25:3116–3118
44. Kato H, Kimura H, Kushima I et al (2023) The genetic architecture of schizophrenia: review of large-scale genetic studies. J Hum Genet 68:175–182
45. Li Y, Li S, Liu J et al (2021) The schizophrenia susceptibility gene NAGA regulates dendritic spine density: further evidence for the dendritic spine pathology of schizophrenia. Mol Psychiatry 26:7102–7104
46. Cheng M-C, Chuang Y-A, Lu C-L et al (2012) Genetic and functional analyses of early growth response (EGR) family genes in schizophrenia. Prog Neuropsychopharmacol Biol Psychiatry 39:149–155
47. Steele-Perkins G, Plachez C, Butz KG et al (2005) The transcription factor gene Nfib is essential for both lung maturation and brain development. Mol Cell Biol 25:685–698
48. Betancourt J, Katzman S, Chen B (2014) Nuclear factor one B regulates neural stem cell differentiation and axonal projection of corticofugal neurons: NFIB regulates cortical development. J Comp Neurol 522:6–35
49. Ma L, Semick SA, Chen Q et al (2020) Schizophrenia risk variants influence multiple classes of transcripts of sorting nexin 19 (SNX19). Mol Psychiatry 25:831–843